AGU PUBLICATIONS

Geophysical Research Letters

RESEARCH LETTER
10.1002/2015GL067536

Key Points:
- Long-lasting (> 20 h) EMIC waves are detected by ground-based magnetometer (near $L \sim 4-6$)
- These EMIC waves have a systematic frequency change with local time
- The local time frequency variation has a clear correlation with the estimated plasmapause location

Correspondence to:
K.-H. Kim,
khan@khu.ac.kr

Citation:
Kim, K.-H., K. Shiokawa, I. R. Mann, J.-S. Park, H.-J. Kwon, K. Hyun, H. Jin, M. Connors (2016), Longitudinal frequency variation of long-lasting EMIC Pc1-Pc2 waves localized in the inner magnetosphere, *Geophys. Res. Lett.*, *43*, 1039–1046, doi:10.1002/2015GL067536.

Received 21 DEC 2015
Accepted 14 JAN 2016
Accepted article online 18 JAN 2016
Published online 15 FEB 2016

Longitudinal frequency variation of long-lasting EMIC Pc1-Pc2 waves localized in the inner magnetosphere

K.-H. Kim[1,2], K. Shiokawa[2], I. R. Mann[3], J.-S. Park[4], H.-J. Kwon[5], K. Hyun[6], H. Jin[1], and M. Connors[7]

[1]School of Space Research, Kyung Hee University, Gyeonggi, Korea, [2]Institute for Space-Earth Environmental Research, Nagoya University, Nagoya, Japan, [3]Department of Physics, University of Alberta, Edmonton, Alberta, Canada, [4]Institute of Space Science, National Central University, Jhongli, Taiwan, [5]Division of Climate Change Research, Korea Polar Research Institute, Incheon, Korea, [6]Korea Meteorological Administration, Seoul, Korea, [7]Centre for Science, Athabasca University, Athabasca, Alberta, Canada

Abstract Long-lasting (> 20 h) electromagnetic ion cyclotron (EMIC) Pc1-Pc2 waves were observed by the Athabasca ($L = \sim 4.6$) induction magnetometer and Canadian Array for Realtime Investigations of Magnetic Activity ($L = \sim 4-6$) fluxgate magnetometers on 5 April 2007. These waves showed a systematic frequency change with local time, the minimum frequency near dusk, and the maximum frequency near dawn. Assuming the plasmapause as a potential source region of the waves, we estimated the plasmapause location from localized proton enhancement (LPE) events observed at NOAA-Polar Orbiting Environmental Satellites and METOP-2 satellites. We found that the longitudinal frequency variation of EMIC waves has a clear correlation with the estimated plasmapause location and that the waves are in the frequency band between the equatorial helium and oxygen gyrofrequencies at the estimated plasmapause. With our analysis results we suggest that the LPE events are caused by wave-particle interaction with the helium band EMIC waves generated near the plasmapause.

1. Introduction

Pc1-Pc2 (frequency = ~0.1–5 Hz) pulsations are commonly observed on the ground at low to high latitudes. It is generally accepted that ground Pc1-Pc2 waves are electromagnetic ion cyclotron (EMIC) waves generated near the magnetospheric equatorial plane through a cyclotron resonant interaction with anisotropic ($T_\perp > T_\parallel$) ions providing free energy for instability [e.g., *Cornwall*, 1965; *Kennel and Petschek*, 1966]. Such anisotropic conditions can be expected during geomagnetically disturbed intervals associated with geomagnetic storms, substorms, and solar wind dynamic pressure variations [e.g., *Fraser and McPherron*, 1982; *Olson and Lee*, 1983; *Ishida et al.*, 1987; *Meredith et al.*, 2003; *Usanova et al.*, 2008].

Theoretical studies have shown that the presence of the cold dense ions and a weak magnetic field are favorable for EMIC wave generation because of the low group velocity of the wave in that region, leading to an enhanced convective growth rate [e.g., *Cornwall*, 1965; *Kennel and Petschek*, 1966; *Kozyra et al.*, 1984]. Thus, the plasmapause and plasmaspheric plumes, in which cold plasmaspheric plasmas overlap with energetic/anisotropic ring current ions on open and closed drift paths, are expected to be favored regions for EMIC wave generation.

According to previous statistical studies [e.g., *Anderson et al.*, 1992a; *Min et al.*, 2012; *Usanova et al.*, 2012], the occurrence rates of EMIC waves increase monotonically with L. That is, EMIC waves occur much more frequently in the outer magnetosphere beyond geosynchronous orbit than in the inner ($L < 6$) magnetosphere. Although previous statistical studies reported a minor enhancement in occurrence near the nominal location of the plasmapause ($L = 4-5$), EMIC waves in the inner magnetosphere play an important role in the dynamics of ring current and radiation belt particles, leading to plasma heating and/or precipitation loss through resonant wave-particle interactions [e.g., *Summers and Thorne*, 2003; *Miyoshi et al.*, 2008; *Usanova et al.*, 2010].

In this paper we present a case study of long-lasting (> 20 h) Pc1-Pc2 waves observed at the Athabasca ($L = \sim 4.6$) and CARISMA ($L = \sim 4-6$) stations in North America on 5 April 2007. These waves are interpreted as EMIC waves generated near $L = \sim 4-6$ in the magnetosphere. The EMIC waves showed a systematic frequency

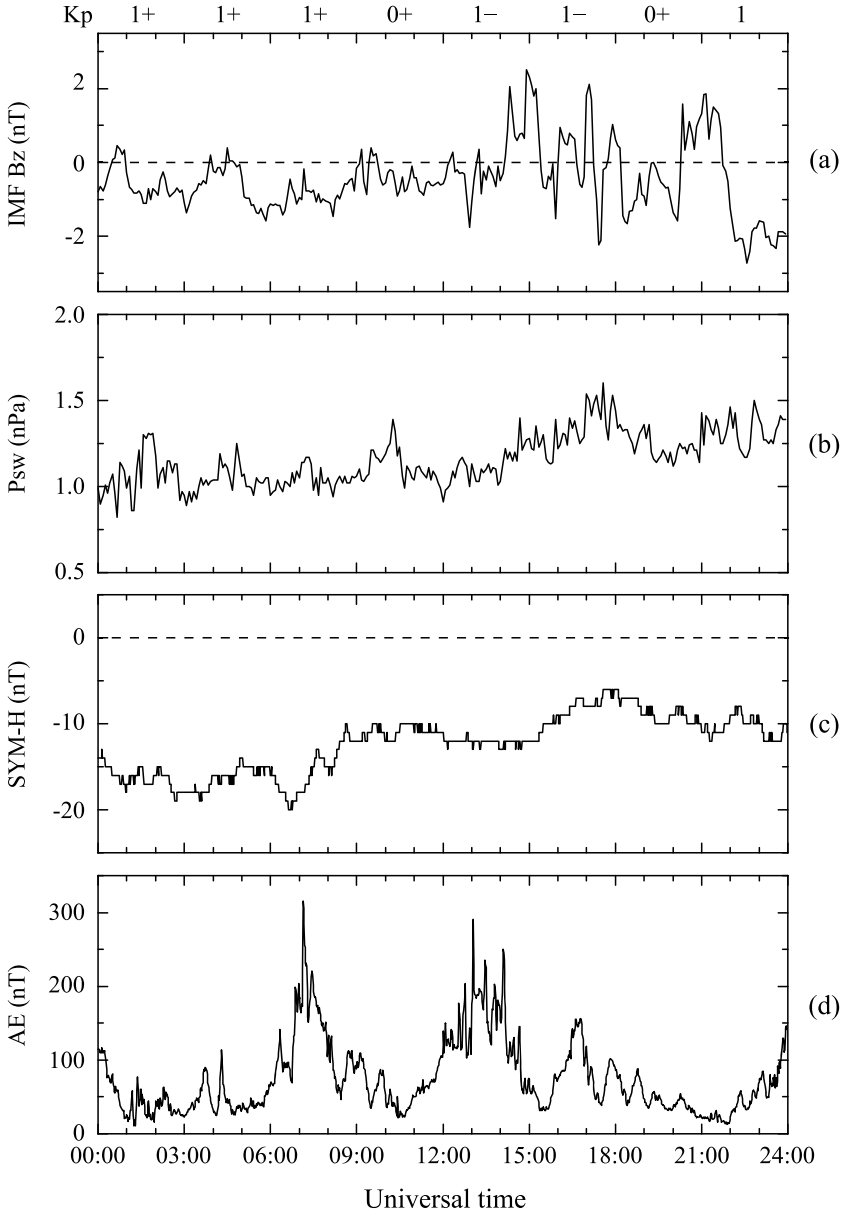

Figure 1. (a) The interplanetary magnetic field (IMF) B_z in the geocentric solar magnetospheric (GSM) coordinate system, (b) the solar wind dynamic pressure (P_{sw}), (c) the *SYM-H* index, and the *AE* index on 5 April 2007. The 3 h values of the K_p index are displayed on the top.

change with longitude although their power was time modulated. We will examine whether the change in frequencies can be associated with the plasmapause location and discuss whether the plasmapause is the source region for the EMIC waves.

2. Observations

Figure 1 shows the interplanetary magnetic field (IMF) B_z in geocentric solar magnetospheric (GSM) coordinates, solar wind dynamic pressure (P_{sw}), *SYM-H* index, and *AE* index for the entire 24 h of 5 April 2007. The 3 h values of the K_p index are displayed on the top of Figure 1a. We note that the geomagnetic conditions shown in Figure 1 were observed during the late recovery phase of a moderate geomagnetic storm with a peak of D_{st} = −63 nT on 1 April 2007. The IMF B_z was primarily southward from 00:00 to 14:00 UT and fluctuated between roughly +2 and −2 nT for 14:00–21:45 UT and then stayed southward until 24:00 UT. On this day P_{sw} exhibited small variations, staying between ~1.0 nPa and ~1.5 nPa. *SYM-H* was about −15 nT near the

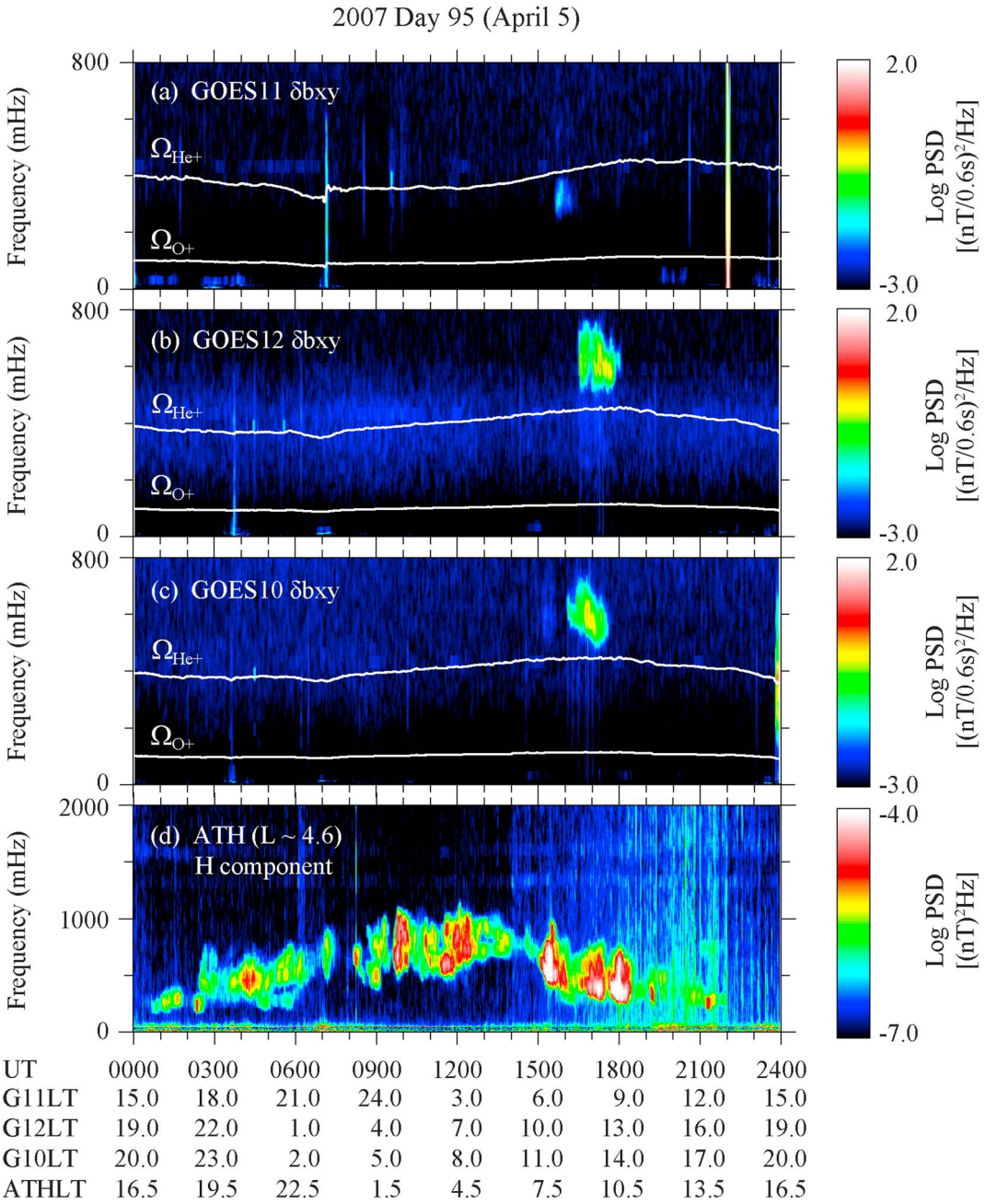

Figure 2. Dynamic power spectra of the transverse field component (δb_{xy}) for the 24 h interval of (a) GOES 11, (b) GOES 12, and (c) GOES 10 magnetometer data on 5 April 2007 in a mean field-aligned (MFA) coordinate system. The transverse power is defined to be in the text. Two white lines indicate the local helium (Ω_{He^+}) and oxygen (Ω_{O^+}) gyrofrequencies, respectively. The magnetic local times of GOES spacecraft are shown at the bottom. (d) The *H* component dynamic spectrum of induction magnetometer at Athabasca (ATH, *L* = ~4.6) in Canada.

beginning of this day, and it gradually increased to −10 nT near the end of the day. *SYM-H* begun to increase around 15:00 UT and reached its maximum, −6 nT, around 18:00 UT. This *SYM-H* increase may be due to the magnetopause current enhancement caused by the enhanced P_{sw} for ~15:00–18:00 UT. The *AE* index shows sudden increases around 07:00 UT and 12:00 UT, indicating substorm expansions, with a peak amplitude of ~300 nT. The IMF B_z, *AE*, and *SYM-H* conditions indicate that the geomagnetic activity on this day was not unusually quiet even though the K_p values were between 0+ and 1+.

Figures 2a–2c show the magnetic field Fourier dynamic spectra of the time-differenced transverse field component (δb_{xy}) for the 24 h interval of GOES 11, GOES 12, and GOES 10 magnetometer data on 5 April 2007

in a mean field-aligned coordinate system [*Hyun et al.*, 2014]. In the δb_{xy} dynamic spectrum, the transverse power is defined to be P_x+P_y, where P_x and P_y are the transverse power spectrum density of δb_x (radial) and δb_y (eastward), respectively. The local time of each GOES spacecraft is given at the bottom. Two white traces included in each panel indicate the local helium (Ω_{He^+}) and oxygen (Ω_{O^+}) gyrofrequencies. In the GOES 11 spectrogram, broadband spectral shapes occurred at ~07:10 UT and ~22:00 UT. The former is associated with the substorm activity as shown in Figure 1c, and the latter is due to a data gap.

The overall intensity in the dynamic spectra at geosynchronous orbit is so low that there are no spectral features in the frequency bands below Ω_{O^+}, between Ω_{O^+} and Ω_{He^+}, and above Ω_{He^+} that stand out above the lower threshold of the color display except for the interval of ~15:30–16:10 UT at GOES 11 and the interval of ~16:00–18:0 UT at GOES 10 and GOES 12. We changed the dynamic range for the display but were unable to find band-limited features similar to those seen under quiet geomagnetic conditions by *Hyun et al.* [2014]. The only prominent band-limited feature is seen above Ω_{He^+} for ~16:00–18:00 UT at GOES 10 and GOES 12 when both spacecraft were near noon. We attribute these transverse wave oscillations to EMIC waves that were generated by changes in the solar wind dynamic pressure. As shown in Figure 1b, P_{sw} increased from ~1 to ~1.5 nPa for the interval of 15:00–18:00 UT.

Figure 2d shows the *H* component dynamic spectrum of the induction magnetometer at Athabasca (ATH, $L = 4.6$) in Canada. Note that the frequency scale of the ATH spectrum is different from that of the GOES spectrum. The local time of ATH is also shown with GOES local times at the bottom of Figure 2. The ATH ground station is longitudinally close to all GOES satellites. The ATH meridian is located between GOES 11 and GOES 12 with a small ground-satellite local time separation within 2.5 h. The ATH spectrum is remarkably different from the GOES magnetic field dynamic spectra. A major feature evident in the ATH spectrum is a band-limited spectral enhancement in Pc1-Pc2 frequency band. This structure lasted more than 20 h from ~01:00 UT to ~21:30 UT with frequencies smoothly changing with longitude. That is, the frequency of Pc1-Pc2 waves changes with local time (LT). It is about 200 mHz at ~01:00 UT near dusk (17.5 LT) and smoothly increases to ~1000 mHz at ~12:00 UT near early dawn (4.5 LT). Then, the frequency shows a gradual decrease to ~250 mHz at ~21:30 UT in the afternoon (14.0 LT). The pulsation power was strong for the ~09:30–12:40 UT and ~15:00–18:30 UT intervals with its level strongly time modulated. The latter interval is concurrent with positive changes in the solar wind dynamic pressure.

Since GOES spacecraft detected enhanced waves in the Pc1-Pc2 frequency band during the interval of slightly increased solar wind pressure, we believe that the very long-lasting Pc1-Pc2 wave activities seen at the ATH ground station at $L = 4.6$ were spatially localized within geosynchronous orbit ($L \sim 6.7$). To infer the latitudinal localization of Pc1-Pc2 wave activity, we examined Canadian Array for Realtime Investigations of Magnetic Activity (CARISMA) fluxgate magnetic field data [*Mann et al.*, 2008]. The longitudinal separation between ATH and CARISMA stations is within ~20°. Fort McMurray (MCMU, $L = 5.35$), Ministik Lake (MSTK, $L = 4.22$), ATH are along the ~307° magnetic meridian, and Fort Churchill (FCHU, $L = 7.44$), Gillam (GILL, $L = 6.15$), Island Lake (ISLL, $L = 5.15$), and Pinawa (PINA, $L = 4.06$) are along the ~330° meridian. The CARISMA and ATH stations are shown on the map in Figure 3a. Figures 3b–3g present Fourier spectrograms of differenced CARISMA *X* (north-south) component fluxgate magnetic field data at MCMU, MSTK, FCHU, GILL, ISLL, and PINA.

Although the spectral power at CARISMA stations cannot make a quantitative comparison with the ATH data because CARISMA data were acquired by fluxgate magnetometers, the spectral shapes at GILL, ISLL, PINA, MCMU, and MSTK are quite similar to that at ATH. During the interval of ~00:30–06:00 UT, the strongest power of Pc1-Pc2 waves was observed at ISLL, and these waves propagated in an ionospheric duct from ISLL to higher latitude stations (FCHU and GILL) and to the lower latitude station (PINA) along the ~330° meridian. The Pc1-Pc2 power at MCMU and MSTK was much weaker than that at GILL, ISLL, and PINA. These observations imply that the Pc1-Pc2 wave activity during ~00:30–06:00 UT occurred at a fixed local time region around ~330° meridian rather than a broad local time region and that the waves originated near a region of $L = \sim 5.2$ in the magnetosphere. Wave activity was the strongest at MSTK for the interval of 09:00–16:00 UT, and these waves were also ducted to a higher station (MCMU). The maximum frequency appeared around 12:00–13:00 UT near dawn (LT = ~5). The wave power was strongly attenuated at the ~330° meridian, implying that the events occurred west of the ~330° meridian near $L = 4.2$. During the interval of ~16:00–19:00 UT, wave activity was stronger at ISLL than at other stations, and Pc1-Pc2 frequency showed local time dependence decreasing from morning to noon.

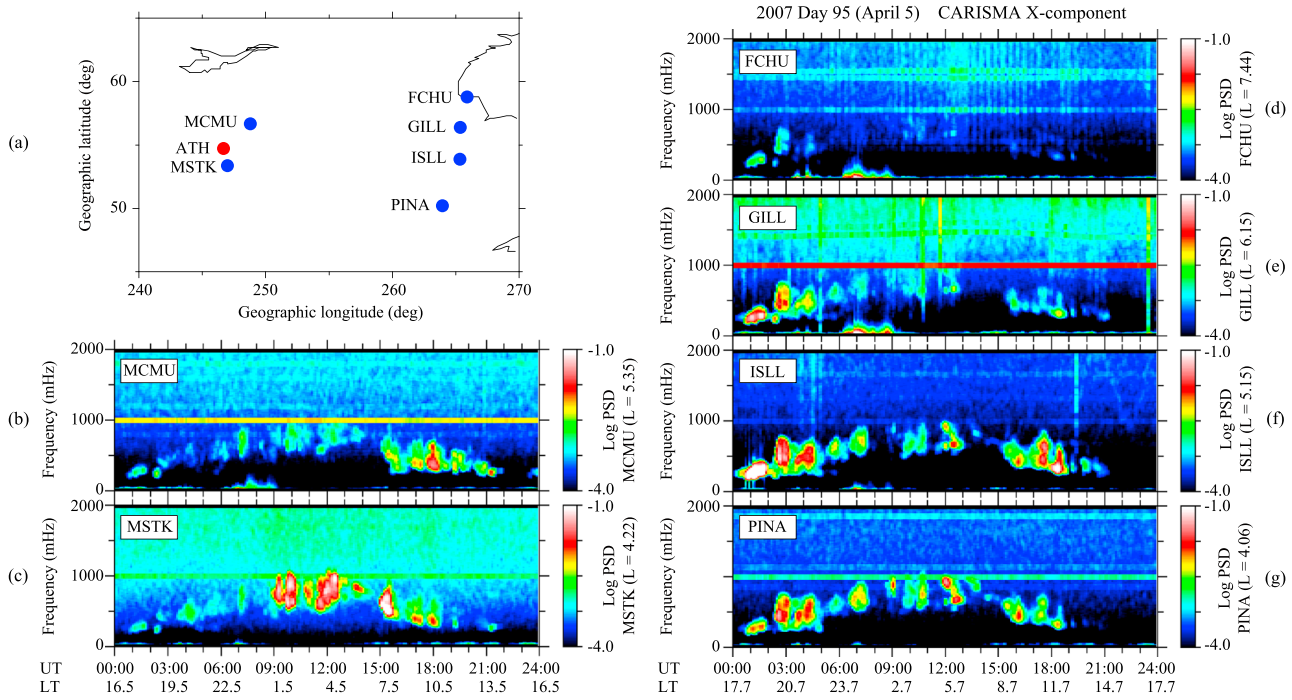

Figure 3. (a) Locations of the selected CARISMA stations and Athabasca station. (b–g) Fourier spectrograms of differenced CARISMA *X* (north-south) component fluxgate magnetic field data from selected CARISMA stations on 5 April 2007.

It has been reported that localized enhancements of energetic (> 30 keV) protons, both trapped at the spacecraft altitude and precipitating, at low altitude in the subauroral region are associated with Pc1 waves [*Yahnina et al.*, 2000]. The localized proton enhancement (LPE) with precipitating particles has been interpreted as strong pitch angle scattering by EMIC waves [e.g., *Miyoshi et al.*, 2008; *Usanova et al.*, 2010; *Hyun et al.*, 2014]. LPE with only trapped particles is also considered to be a very weak pitch angle diffusion [*Yahnina et al.*, 2000]. Thus, EMIC source region can be estimated from LPE. We examine whether such LPE events occurred during the interval of Pc1-Pc2 waves observed at ATH and CARISMA stations.

Figure 4 shows the trapped (blue) and precipitating (red) proton count rates in the 30–80 keV channel measured by the Medium Energy Proton and Electron Detector (MEPED) instrument instrument on the low-altitude polar-orbiting METOP-2 spacecraft. METOP-2 encountered the isotropic zone, in which the trapped and precipitating count rates are comparable, around 03:30:27 UT as passing Northern Hemisphere higher (auroral) latitudes (Figure 4a). This isotropic particle distribution is due to the pitch angle scattering of protons bouncing between mirror points along the magnetospheric magnetic field stretched on the nightside [e.g., *Sergeev et al.*, 1983]. During the interval equatorward of this isotropic zone, the protons show highly anisotropic distributions with a very weak precipitation of energetic protons. Inside the anisotropic zone,

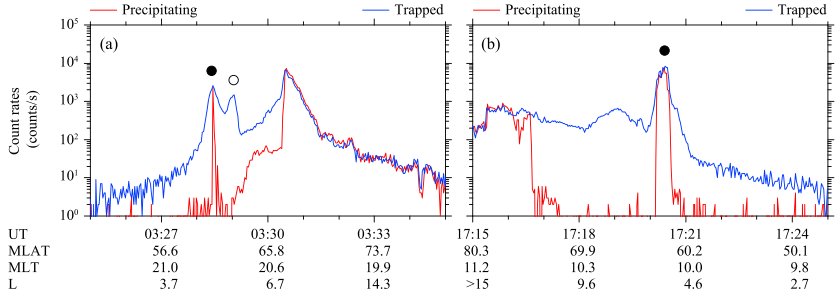

Figure 4. The trapped (blue) and precipitating (red) proton count rates in the 30–80 keV channel measured by MEPED instrument on the low-altitude polar-orbiting METOP-2 spacecraft for the intervals of (a) 03:26–03:35 UT and (b) 17:15–17:25 UT on 5 April 2007. Solid and open circles indicate localized proton enhancement with and without precipitating protons, respectively.

METOP-2 detected isolated peaks in the proton count rates (i.e., LPEs) at 03:28:27 UT (marked by solid circles) and 03:30:27 UT (marked by open circles) in the premidnight sector. The former was observed at L = ~4.8, MLT = 20.9, and MLAT = 61.1° N with both trapped and precipitating particles, and the latter was observed at L = ~5.4, MLT = 20.8, and MLAT = 62.7° N with only the enhancement of trapped particles. The local time difference between CARISMA and METOP-2 when LPEs were observed was ~0.5 h. As shown above, the strongest Pc1-Pc2 wave activity for ~03:00–04:00 UT was observed at ISLL (L = 5.15), which was very close to the L shell of LPE events. Figure 4b shows another LPE event with strong precipitating protons at 17:20:25 UT. This event was observed in the morning sector (L = ~5.1, MLT = 10.0, and MLAT = 61.9° N). The L shell of the LPE is nearly equal to that of ISLL with a small local time separation (~1.0 h). These observations support that the occurrence of LPEs is strongly related with EMIC waves, seen as Pc1-Pc2 waves on the ground.

3. Discussion

Early studies for LPE reported that the region of LPE is located just inside the plasmapause [*Cornwall et al.*, 1971; *Williams and Lyons*, 1974] or outside the plasmapause [*Mizera*, 1974; *Søraas and Berg*, 1974]. It has been suggested that the equatorial region of the magnetosphere is favored for EMIC wave generation because of the low group velocity of the wave in that region, leading to enhancement of the convective growth rate [e.g., *Cornwall*, 1965; *Kennel and Petschek*, 1966; *Kozyra et al.*, 1984]. Thus, the growth rate of EMIC waves may reach a maximum at the inner edge of the plasmapause and the outer magnetosphere at high L where group velocity is low [e.g., *Perraut et al.*, 1976; *Kozyra et al.*, 1984]. This indicates that LPEs can be observed both inside and outside the plasmapause because EMIC waves have been generated over a wide L range [e.g., *Anderson et al.*, 1992a]. The LPEs shown in Figure 4 were magnetically mapped to the ground at L = ~5 where strong Pc1-Pc2 waves were seen. These LPE events, in conjunction with Pc1-Pc2 waves, have been interpreted to be the result of wave-particle interactions with EMIC waves enhanced near L = ~5, the typical location of the plasmapause [e.g., *Yahnina et al.*, 2000; *Yahnin and Yahnina*, 2007; *Miyoshi et al.*, 2008; *Usanova et al.*, 2010].

Fraser et al. [1989] demonstrated that the source region of Pc1 pulsations observed at middle and low-latitude ground stations is just inside the plasmapause identified at L = ~4.9. In their study linear convective wave growth was calculated by using the parameters observed and assuming a location just inside the plasmapause at L= 4.7. This showed the presence of growing waves in the helium band between helium and oxygen gyrofrequencies. *Thorne et al.* [2013] showed that EMIC waves below the helium gyrofrequency near L = 4 just inside the plasmapause effectively scatter protons at energies of ~10–100 keV. *Sakaguchi et al.* [2008] reported that isolated proton arcs at subauroral latitudes appeared coincident with strong Pc1 waves in the helium band. *Yahnin et al.* [2013] reported that the subauroral source is located in the vicinity of the plasmapause or in the cold plasma gradient inside the plasmapause.

We suggest that the source region of our long-lasting Pc1-Pc2 waves is near the plasmapause. The longitudinal variation of Pc1-Pc2 frequencies seen on the ground may be due to the spatial and/or temporal variation of plasmapause location. That is, the farther plasmapause distance is near dusk (~02:00 UT), and the closer distance is near early dawn (~12:00 UT). We can make a rough estimate of the plasmapause location assuming that LPEs are produced by wave-particle interactions with EMIC waves generated near the plasmapause.

We used three NOAA-Polar Orbiting Environmental Satellites (POES) (NOAA-15, NOAA-16, and NOAA-18) and METOP-02 satellites to identify L values of LPEs on 5 April 2007. Only LPE events observed within 2 h of local time of CARISMA stations are plotted in Figure 5a. Red and Blue dots indicate LPE events with and without precipitating protons, respectively. The radial location of LPEs shows a systematic variation with UT (and thus LT). That is, the L values from 01:00 to 03:00 UT (~18–19 LT) are larger than those from 11:00 to 13:00 UT (~4–5 LT). From 17:00 to 19:00 UT near noon, LPE events with precipitation were detected in a wide range, L = ~5–9. We note that there was a slight P_{sw} enhancement from 15:00 to 19:00 UT and GOES spacecraft detected EMIC waves for the interval of 16:00–18:00 UT. Therefore, we suggest that EMIC waves were generated over a wide L range for the interval of 17:00–19:00 UT.

To make an estimate of the plasmapause location using LPE events, the second order polynomial fit was applied to the LPE data points from 00:00 to 15:00 UT and is plotted with a smoothed curve in Figure 5a. Although the LPE events from 16:00 to 21:00 UT were not used for the polynomial fit because of a large scatter in L, some of LPE events lie closely below and above the fitting line. The polynomial exhibits a minimum of L = ~4.6 at 11:30 UT (~4 LT) and a maximum of L = ~7.3 at 23:30 UT (~16 LT). This indicates that the estimated

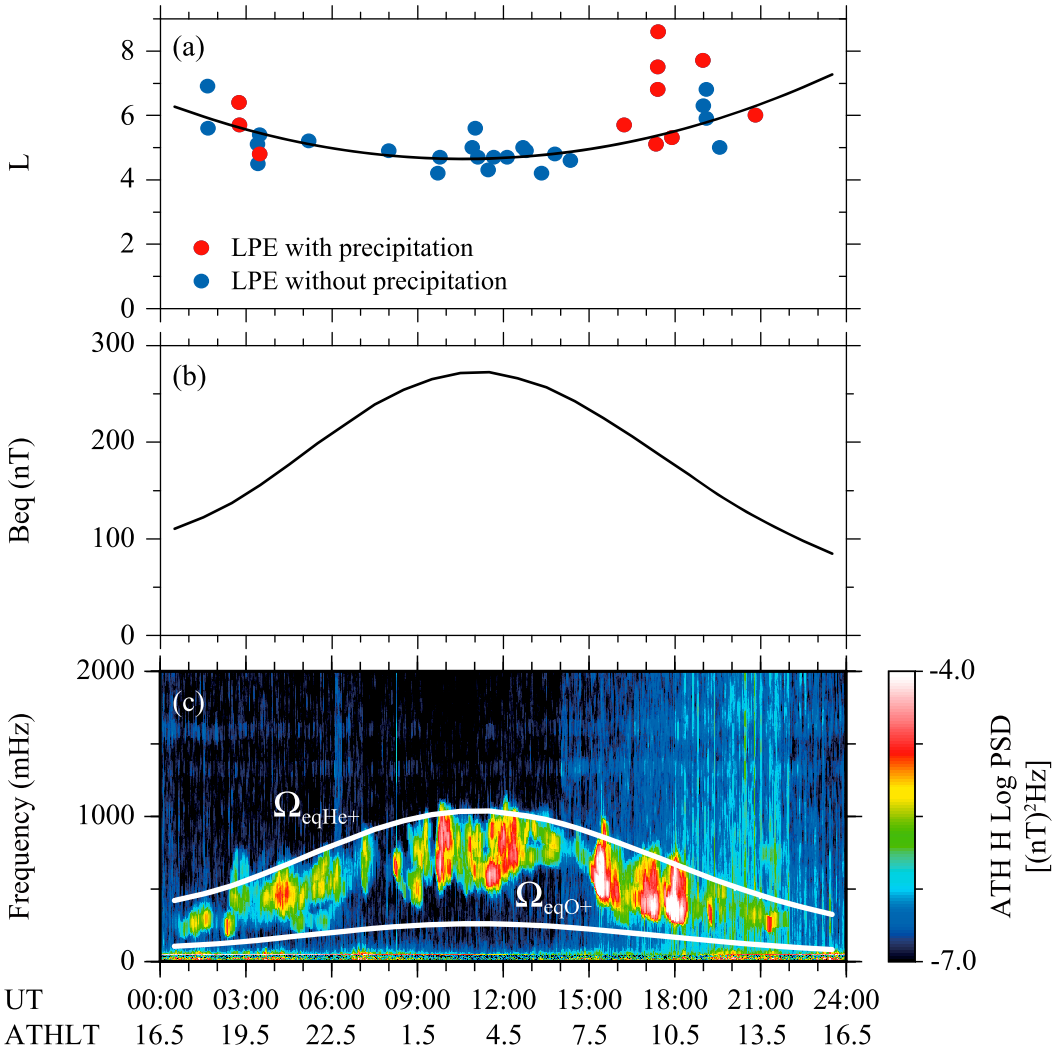

Figure 5. (a) Localized proton enhancement (LPE) events observed within 2 h of local time of CARISMA stations by 3 NOAA-POES satellites (NOAA-15, NOAA-16, and NOAA-18) and METOP-02 on 5 April 2007. Red and blue dots indicate LPE events with and without precipitating protons, respectively. A smooth curve indicates the second order polynomial fit to the LPE data points from 00:00 to 15:00 UT. (b) The equatorial magnetic field intensity (B_{eq}) given by the TS05 model at the estimated plasmapause location. (c) The *H* component dynamic spectrum of Athabasca (ATH) induction magnetometer data. Two white lines indicate the equatorial helium (Ω_{eqHe^+}) and oxygen (Ω_{eqO^+}) gyrofrequencies, respectively.

plasmapause is asymmetric along the local time [e.g., *Kwon et al.*, 2015]. However, we do not exclude temporal variations of the plasmapause location because of IMF conditions and geomagnetic activities (see Figure 1).

Figure 5b shows the equatorial magnetic field intensity (B_{eq}) given by the TS05 model [*Tsyganenko and Sitnov*, 2005] at the estimated plasmapause location. From the B_{eq} profile, we calculated the helium (Ω_{eqHe^+}) and oxygen (Ω_{eqO^+}) gyrofrequencies at the equatorial plasmapause, and the result is shown in Figure 5c with the *H* component dynamic spectrum of ATH. The general trend of the longitudinal variation of the estimated equatorial gyrofrequencies is similar to the band structure of Pc1-Pc2 waves seen in the dynamic spectrum. Most of the wave power shows in the frequency band between Ω_{eqHe^+} and Ω_{eqO^+} (i.e., the helium band), which gives support to previous theoretical and observational studies [e.g., *Fraser et al.*, 1989; *Sakaguchi et al.*, 2008; *Thorne et al.*, 2013]. We believe that the LPE events result from wave-particle interaction with the helium band EMIC waves generated near the plasmapause.

Considering the plasmapause as a possible source region, we examined the longitudinal frequency variation of Pc1-Pc2 waves localized in the inner magnetosphere and showed a clear correlation between frequency

variation and the estimated plasmapause location. We cannot confirm a systematic local time frequency change, similar to our observations, of EMIC waves near the typical location of the plasmapause at $L = 4–5$ in a previous study [*Anderson et al.*, 1992b]. This may be due to the fact that the plasmapause location is dynamic. Thus, we wish to emphasize that it is necessary to know the location of the plasmapause for various geomagnetic conditions in order to understand the contribution of the plasmapause to EMIC wave generation. In the future work, we will perform statistical analyses to examine the relationship between EMIC wave frequency and the plasmapause location using the data from Van Allen Probes.

Acknowledgments
The high time resolution GOES magnetic field data used in this study were obtained from the coordinated data analysis web (http://cdaweb.gsfc.nasa.gov/cdaweb). K_p, *AE*, and *SYM-H* were obtained from the World Data Center C2 (WDC-C2) for Geomagnetism, Kyoto University (http://wdc.kugi.kyoto-u.ac.jp). The interplanetary magnetic field and solar wind data were provided from OMNI Web (http://omniweb.gsfc.nasa.gov/). The MetOp and NOAA/POES particle data were obtained from NOAA National Geophysical Data Center (http://ngdc.noaa.gov). The authors thank D.K. Milling and the rest of the CARISMA team for the data. CARISMA is operated by the University of Alberta, funded by the Canadian Space Agency. K.-H. Kim is grateful to H. Kawano for the valuable comments. This work was supported by the Basic Science Research Program by NRF-2013R1A1A2A10004414 and by BK21+ through the National Research Foundation (NRF) funded by the Ministry of Education of Korea. Work of K.-H. Kim was also supported by project PE15090 of the Korea Polar Research Institute. This work was supported by JSPS KAKENHI grant 15H05815.

References

Anderson, B. J., R. E. Erlandson, and L. J. Zanetti (1992a), A statistical study of Pc 1–2 magnetic pulsations in the equatorial magnetosphere: 1. Equatorial occurrence distributions, *J. Geophys. Res.*, *97*(A3), 3075–3088, doi:10.1029/91JA02706.

Anderson, B. J., R. E. Erlandson, and L. J. Zanetti (1992b), A statistical study of Pc 1–2 magnetic pulsations in the equatorial magnetosphere: 2. Wave properties, *J. Geophys. Res.*, *97*(A3), 3089–3101, doi:10.1029/91JA02697.

Cornwall, J. M. (1965), Cyclotron instabilities and electromagnetic emission in the ultra low frequency and very low frequency ranges, *J. Geophys. Res.*, *70*(1), 61–69, doi:10.1029/JZ070i001p00061.

Cornwall, J. M., H. H. Hilton, and P. F. Mizera (1971), Observations of precipitating protons in the energy range 2.5 kev $\leq$ E $\leq$ 200 kev, *J. Geophys. Res.*, *76*(22), 5220–5234.

Fraser, B. J., and R. L. McPherron (1982), Pc 1–2 magnetic pulsation spectra and heavy ion effects at synchronous orbit: ATS 6 results, *J. Geophys. Res.*, *87*(A6), 4560–4566, doi:10.1029/JA087iA06p04560.

Fraser, B. J., W. J. Kemp, and D. J. Webster (1989), Ground-satellite study of a Pc 1 ion cyclotron wave event, *J. Geophys. Res.*, *94*(A0), 11,855–11,863.

Hyun, K., K.-H. Kim, E. Lee, H.-J. Kwon, D.-H. Lee, and H. Jin (2014), Loss of geosynchronous relativistic electrons by EMIC wave scattering under quiet geomagnetic conditions, *J. Geophys. Res. Space Physics*, *119*, 8357–8371, doi:10.1002/2014JA020234.

Ishida, J., S. Kokubun, and R. L. McPherron (1987), Substorm effects on spectral structures of Pc 1 waves at synchronous orbit, *J. Geophys. Res.*, *92*(A1), 143–158.

Kennel, C. F., and H. E. Petschek (1966), Limit on stably trapped particle fluxes, *J. Geophys. Res.*, *71*(1), 1–28.

Kozyra, J. U., T. E. Cravens, F. Nagy, E. G. Fontheim, and R. S. B. Ong (1984), Effects of energetic heavy ions on electromagnetic ion cyclotron wave generation in the plasmapause region, *J. Geophys. Res.*, *89*(A4), 2217–2233, doi:10.1029/JA089iA04p02217.

Kwon, H.-J., K.-H. Kim, G. Jee, J.-S. Park, H. Jin, and Y. Nishimura (2015), Plasmapause location under quiet geomagnetic conditions (Kp $\leq$ 1): THEMIS observations, *Geophys. Res. Lett.*, *42*, doi:10.1002/2015GL066090.

Mann, I. R., et al. (2008), The upgraded CARISMA magnetometer array in the THEMIS Era, *Space Sci. Rev.*, *141*, 413–451, doi:10.1007/s11214-008-9457-6.

Meredith, N. P., R. M. Thorne, R. B. Horne, D. Summers, B. J. Fraser, and R. R. Anderson (2003), Statistical analysis of relativistic electron energies for cyclotron resonance with EMIC waves observed on CRRES, *J. Geophys. Res.*, *108*(A6), 1250, doi:10.1029/2002JA009700.

Min, K., J. Lee, K. Keika, and W. Li (2012), Global distribution of EMIC waves derived from THEMIS observations, *J. Geophys. Res.*, *117*, A05219, doi:10.1029/2012JA017515.

Miyoshi, Y., K. Sakaguchi, K. Shiokawa, D. Evans, J. Albert, M. Connors, and V. Jordanova (2008), Precipitation of radiation belt electrons by EMIC waves, observed from ground and space, *Geophys. Res. Lett.*, *35*, L23101, doi:10.1029/2008GL035727.

Mizera, P. F. (1974), Observations of precipitating protons with ring current energies, *J. Geophys. Res.*, *79*(4), 581–588.

Olson, J. V., and L. C. Lee (1983), Pc1 wave generation by sudden impulses, *Planet. Space Sci.*, *31*(3), 295–302, doi:10.1016/0032-0633(83)90079-X.

Perraut, S., R. Gendrin, and A. Roux (1976), Amplification of ion-cyclotron waves for various typical radial profiles of magnetospheric parameters, *J. Atmos. Terr. Phys.*, *38*, 1191–1199.

Sakaguchi, K., K. Shiokawa, Y. Miyoshi, Y. Otsuka, T. Ogawa, K. Asamura, and M. Connors (2008), Simultaneous appearance of isolated auroral arcs and Pc 1 geomagnetic pulsations at subauroral latitudes, *J. Geophys. Res.*, *113*, A05201, doi:10.1029/2007JA012888.

Sergeev, V. A., E. Sazhina, N. Tsyganenko, J. Lundblad, and F. Soraas (1983), Pitch angle scattering of energetic protons in the magnetotail current sheet as the dominant source of their isotropic precipitation into the nightside ionosphere, *Planet. Space Sci.*, *31*, 1147–1155.

Søraas, F., and L. E. Berg (1974), Correlated satellite measurements of proton precipitation and plasma density, *J. Geophys. Res.*, *79*, 5171–5180.

Summers, D., and R. M. Thorne (2003), Relativistic electron pitch-angle scattering by electromagnetic ion cyclotron waves during geomagnetic storms, *J. Geophys. Res.*, *108*(A4), 1143, doi:10.1029/2002JA009489.

Thorne, R. M., R. B. Horne, V. K. Jordanova, J. Bortnik, and S. A. Glauert (2013), Interaction of EMIC waves with thermal plasma and radiation belt particles, in *Magnetospheric ULF Waves: Synthesis and New Directions, Geophys. Monogr. Ser.*, vol. 169, edited by K. Takahashi, pp. 213–223, AGU, Washington, D. C.

Tsyganenko, N. A., and M. I. Sitnov (2005), Modeling the dynamics of the inner magnetosphere during strong geomagnetic storms, *J. Geophys. Res.*, *110*, A03208, doi:10.1029/2004JA010798.

Usanova, M. E., I. R. Mann, I. J. Rae, Z. C. Kale, V. Angelopoulos, J. W. Bonnell, K. H. Glassmeier, H. U. Auster, and H. J. Singer (2008), Multipoint observations of magnetospheric compression-related EMIC Pc1 waves by THEMIS and CARISMA, *Geophys. Res. Lett.*, *35*, L17S25, doi:10.1029/2008GL034458.

Usanova, M. E., et al. (2010), Conjugate ground and multisatellite observations of compression-related EMIC Pc1 waves and associated proton precipitation, *J. Geophys. Res.*, *115*, A07208, doi:10.1029/2009JA014935.

Usanova, M. E., I. R. Mann, J. Bortnik, L. Shao, and V. Angelopoulos (2012), THEMIS observations of electromagnetic ion cyclotron wave occurrence: Dependence on AE, SYMH, and solar wind dynamic pressure, *J. Geophys. Res.*, *117*, A10218, doi:10.1029/2012JA018049.

Yahnina, T. A., A. G. Yahnin, J. Kangas, and J. Manninen (2000), Proton precipitation related to Pc1 pulsations, *Geophys. Res. Lett.*, *27*(21), 3575–3578.

Yahnin, A. G., and T. A. Yahnina (2007), Energetic proton precipitation related to ion.cyclotron waves, *J. Atmos. Terr. Phys.*, *69*, 1690–1706.

Yahnin, A. G., T. A. Yahnina, H. Frey, and V. Pierrard (2013), Sub-oval proton aurora spots: Mapping relatively to the plasmapause, *J. Atmos. Terr. Phys.*, *99*, 61–66.

Williams, D. J., and L. R. Lyons (1974), The proton ring current and its interaction with the plasmapause: Storm recovery phase, *J. geophys. Res.*, *79*, 4195–4207.